EJNMMI Research
a SpringerOpen Journal

ORIGINAL RESEARCH Open Access

Pharmacokinetic modeling of P-glycoprotein function at the rat and human blood–brain barriers studied with (*R*)-[^{11}C]verapamil positron emission tomography

Julia Müllauer[1], Claudia Kuntner[1], Martin Bauer[2], Jens P Bankstahl[3], Markus Müller[2], Rob A Voskuyl[4,5], Oliver Langer[1,2] and Stina Syvänen[5,6*]

Abstract

Background: This study investigated the influence of P-glycoprotein (P-gp) inhibitor tariquidar on the pharmacokinetics of P-gp substrate radiotracer (*R*)-[^{11}C]verapamil in plasma and brain of rats and humans by means of positron emission tomography (PET).

Methods: Data obtained from a preclinical and clinical study, in which paired (*R*)-[^{11}C]verapamil PET scans were performed before, during, and after tariquidar administration, were analyzed using nonlinear mixed effects (NLME) modeling. Administration of tariquidar was included as a covariate on the influx and efflux parameters (Q_{in} and Q_{out}) in order to investigate if tariquidar increased influx or decreased outflux of radiotracer across the blood–brain barrier (BBB). Additionally, the influence of pilocarpine-induced status epilepticus (SE) was tested on all model parameters, and the brain-to-plasma partition coefficient ($V_{T\text{-}NLME}$) was calculated.

Results: Our model indicated that tariquidar enhances brain uptake of (*R*)-[^{11}C]verapamil by decreasing Q_{out}. The reduction in Q_{out} in rats during and immediately after tariquidar administration (sevenfold) was more pronounced than in the second PET scan acquired 2 h after tariquidar administration (fivefold). The effect of tariquidar on Q_{out} in humans was apparent during and immediately after tariquidar administration (twofold reduction in Q_{out}) but was negligible in the second PET scan. SE was found to influence the pharmacological volume of distribution of the central brain compartment V_{br1}. Tariquidar treatment lead to an increase in $V_{T\text{-}NLME}$, and pilocarpine-induced SE lead to increased (*R*)-[^{11}C]verapamil distribution to the peripheral brain compartment.

Conclusions: Using NLME modeling, we were able to provide mechanistic insight into the effects of tariquidar and SE on (*R*)-[^{11}C]verapamil transport across the BBB in control and 48 h post SE rats as well as in humans.

Keywords: Nonlinear mixed effects modeling, Positron emission tomography, (*R*)-[^{11}C]verapamil, P-glycoprotein, Tariquidar, Pilocarpine-induced epilepsy, Species differences

* Correspondence: stina.syvanen@pubcare.uu.se
[5]Division of Pharmacology, Leiden University, Einsteinweg 55, Leiden 2333 CC, The Netherlands
[6]Department of Public Health and Caring Sciences, Uppsala University, Rudbecklaboratoriet, Uppsala 751 85, Sweden
Full list of author information is available at the end of the article

Springer

© 2012 Müllauer et al.; licensee Springer. This is an Open Access article distributed under the terms of the Creative Commons Attribution License (http://creativecommons.org/licenses/by/2.0), which permits unrestricted use, distribution, and reproduction in any medium, provided the original work is properly cited.

Background

About one-third of patients with epilepsy are pharmacoresistant and do not respond adequately to antiepileptic drug therapy [1]. The blood–brain barrier (BBB) has a major role in regulating the transport of antiepileptic drugs to their target site of action. Drug penetration across the BBB is influenced by several mechanisms, such as passive diffusion, active influx, and active efflux. Regional overactivity of efflux transporters at the BBB is thought to contribute to drug resistance by impeding therapeutically effective concentrations of antiepileptic drugs at their sites of action [2]. P-glycoprotein (P-gp), which is physiologically located at the luminal membrane of brain capillary endothelial cells, is currently one of the most widely studied efflux transporters at the BBB. Positron emission tomography (PET) with carbon-11-labeled P-gp substrates, such as (*R*)-[^{11}C]verapamil or [^{11}C]-*N*-desmethyl-loperamide, has been evaluated as a tool for *in vivo* imaging of P-gp function in different species [3-6]. However, these radiotracers are high-affinity P-gp substrates and consequently display very low brain concentrations, limiting their suitability as PET tracers [5,7,8]. This drawback can be overcome by modulation of P-gp with the third-generation P-gp inhibitor tariquidar, which leads to increased brain uptake of these radiotracers. After partial inhibition of P-gp with 3 mg/kg tariquidar, regional differences in P-gp expression and functionality between naïve and status epilepticus (SE) rats become evident [9,10]. Additionally, P-gp at the BBB has been found to be upregulated after acute seizure activity like SE or in chronic epilepsy [11-15]. Further, species-dependent differences in P-gp expression and functionality at the BBB have been described and discussed in literature [16-18], including the P-gp mediated interaction between (*R*)-[^{11}C]verapamil and tariquidar at the human and rat BBB studied by Bauer et al. [18]. Despite several published studies, there is still an ongoing debate, whether P-gp inhibition with tariquidar or other inhibitors is enhancing the brain uptake of substrate radiotracers by increasing the influx or decreasing outflux across the BBB of the radiotracer [9].

In PET research, pharmacokinetic (PK) modeling (compartment modeling) is used for detailed quantitative analysis of PET data. Each individual is analyzed separately, and group averages and variability are subsequently based on the individual estimates. An alternative way to analyze PK-pharmacodynamic (PD) data is nonlinear mixed effects (NLME) modeling, often referred to as population modeling. This modeling approach is routinely used in pharmaceutical research and has also found to be suitable for PET research [19-29]. A population approach analyzes data from all subjects simultaneously and gives a description of the PK in the typical subject as well as the variation in the study population. Syvänen et al. [26] analyzed data from a (*R*)-[^{11}C]verapamil PET study in naïve and post SE rats (seven days after kainate treatment) with both a PET PK-modeling approach and a NLME-modeling approach and concluded that both approaches produced similar PK parameter estimates, but that NLME modeling provided more precise parameter estimates.

In the present study, we analyzed data obtained from a preclinical PET study in naïve rats and rats at 48 h after pilocarpine-induced SE [9] and a clinical study in healthy volunteers [30]. In both studies, subjects underwent paired (*R*)-[^{11}C]verapamil PET scans before, during, and after administration of tariquidar (rats, 3 and 15 mg/kg; humans, 2 mg/kg) (see Figure 1). Tariquidar was administered during the first PET scan and PET data acquisition continued during and after tariquidar administration. Both in rats and in humans a pronounced and immediate increase in (*R*)-[^{11}C]verapamil brain uptake during treatment with tariquidar was observed. In the original analysis of the rat data [9], (*R*)-[^{11}C]verapamil brain curves obtained during and after tariquidar treatment in the first PET scan (60 to 140 min) were not included in PET PK modeling as standard PET approaches do not handle this type of data. In the original analysis of the human data [30], however, efforts were made to analyze the time course of the effect of tariquidar administration on activity in brain during the first PET scan using an indirect response PK-PD model proposed by Syvänen et al. [31] (see supplemental data of Wagner et al. [30]). These results suggested that the (*R*)-[^{11}C]verapamil brain curves obtained during and immediately following tariquidar treatment may contain important information that may contribute to the model structure and parameter outcome. Therefore, we hypothesized that the use of NLME modeling may provide mechanistic information of the PK of (*R*)-[^{11}C]verapamil in plasma and brain including quantification of the influence of tariquidar-induced P-gp inhibition and pilocarpine-induced SE on (*R*)-[^{11}C]verapamil brain and plasma PK. The specific aims of this study were to investigate whether the observed increase in (*R*)-[^{11}C]verapamil brain uptake during and immediately after tariquidar treatment influences PK model parameter estimates and if regional differences in certain brain regions as recently discussed by Bankstahl et al. [9] become more pronounced when these data are included in the analysis. Additionally, it was studied whether the enhancement of brain uptake of (*R*)-[^{11}C]verapamil after tariquidar administration was caused by increased influx or decreased outflux of the radiotracer. Finally, the developed model based on the rat dataset was applied to the human data set to identify potential species differences in P-gp function.

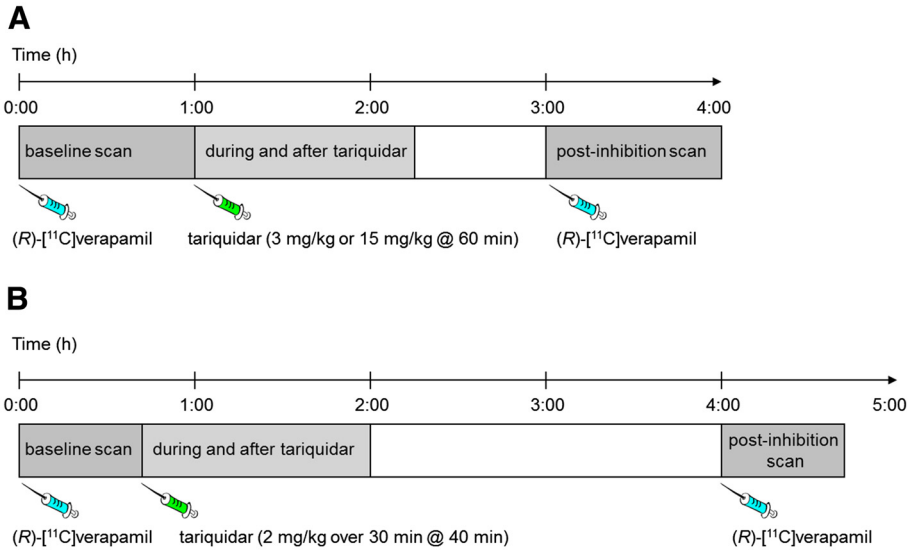

Figure 1 Scheme of the setups for the preclinical study (A) and the clinical study (B).

Methods

Preclinical data set

The preclinical dataset was recently published by Bankstahl et al. [9], and the study setup is illustrated in Figure 1A. The study was approved by the Institutional Animal Care and Use Committee, and all study procedures were performed in accordance with the European Communities Council Directive of November 24, 1986 (86/609/EEC). All efforts were made to minimize both the suffering and the number of animals used in this study.

Naïve control (n = 11) and 48-h post SE (n = 10) female Sprague–Dawley rats (Harlan Nederland, Horst, Netherlands) weighing 260±28 g underwent paired (*R*)-[^{11}C]verapamil PET scans. The number of animals, animal weights, injected doses, and injection times of all treatment groups are summarized in Table 1. All rats underwent a 140-min dynamic baseline PET scan starting simultaneously with (*R*)-[^{11}C]verapamil administration given as an intravenous bolus (I.V.) on a micro-PET Focus 220 scanner (Medical Solutions, Siemens Knoxville, TN, USA). Tariquidar (3 or 15 mg/kg) was administered at 60 min after the start of the baseline scan as an I.V. bolus over 60 sec. A second 60-min dynamic (*R*)-[^{11}C]verapamil PET scan, referred to as post-inhibition scan, was started 2 h after tariquidar administration. In parallel to the measurement of (*R*)-[^{11}C]verapamil brain concentrations with PET, (*R*)-[^{11}C]verapamil concentration in blood and plasma (mean plasma-to-blood ratio of (*R*)-[^{11}C]verapamil = 1.29±0.10 [32]) was obtained with continuous arterial blood sampling. In addition, (*R*)-[^{11}C]verapamil concentration in plasma was corrected for radiolabelled metabolites. More information on the PET scan procedure, the study setup, the arterial blood sampling, and the metabolite correction can be found in the previously published

Table 1 Number of animals (n), weight at time of PET, injected doses (average ± standard deviation) of (*R*)-[^{11}C]verapamil for baseline and post-inhibition scans in naïve and 48-h post SE rats and different treatments with 3 or 15 mg/kg of tariquidar

	Naïve and 3 mg/kg tariquidar treated	Naïve and 15 mg/kg tariquidar treated	48-h post SE and 3 mg/kg tariquidar treated	48-h post SE and 15 mg/kg tariquidar treated	All groups
N	7	4	5	5	21
Body weight (g)	260 ± 5	307 ± 18	234 ± 14	247 ± 16	260 ± 28
Baseline (*R*)-[^{11}C]verapamil (MBq)	97 ± 27	88 ± 17	84 ± 20	94 ± 25	91 ± 22
I.V. injection time (sec)	18 ± 7	39 ± 10	19 ± 2	25 ± 11	24 ± 11
Post-inhibition (*R*)-[^{11}C]verapamil (MBq)	93 ± 27	101 ± 28	91 ± 9	92 ± 16	94 ± 21
I.V. injection time (sec)	18 ± 6	36 ± 5	16 ± 2	32 ± 18	24 ± 13

studies by Bankstahl et al. [9] and Kuntner et al. [10]. For modeling, (*R*)-[^{11}C]verapamil concentration-time curves before and after tariquidar administration, expressed in units of kilobecquerels per milliliters (kBq/ml), were extracted from eight brain regions of interest (whole brain (WB), corpus striatum (CS), entorhinal cortex (EC), septal hippocampus (Shipp), temporal hippocampus (THipp), thalamus (Th), cerebellum (Cer), and frontal motor cortex (FMC)) as described previously [10]. For comparison with human data, activity concentrations were normalized to injected activity per body weight and expressed as standardized uptake value (SUV).

Clinical data set

The clinical dataset has been described in detail by Wagner et al. [30]. The study setup is illustrated in Figure 1B. The study protocol was approved by the local Ethics Committee and was performed in accordance with the Declaration of Helsinki (1964) in the revised version of 2000 (Edinburgh), the Guidelines of the International Conference of Harmonization, the Good Clinical Practice Guidelines, and the Austrian Drug Law (Arzneimittelgesetz). All subjects were given a detailed description of the study, and their written consent was obtained before they enrolled in the study.

Five healthy male volunteers with an average age of 32±8 years and an average body weight of 74±5 kg underwent paired (*R*)-[^{11}C]verapamil PET scans of 120- and 40-min duration, respectively, with an interval of 2 h between the two scans on an Advance PET scanner (GE Medical Systems, Waukesha, WI, USA). Dynamic PET and arterial blood sampling were started at the time of radiotracer injection. Forty minutes after the start of the baseline scan, tariquidar was administered at a dose of 2 mg/kg of body weight I.V. over 30 min. Post-inhibition scan was performed at 2 h and 50 min after the end of tariquidar infusion. Number of participants, body weight, injected doses, and radiotracer injection times are summarized in Table 2.

For modeling, (*R*)-[^{11}C]verapamil concentration-time curves before and after tariquidar administration, expressed in kBq/ml, were extracted from a WB gray matter region as described previously [30].

PK modeling: PET approach

PET PK modeling parameters for rats and human were taken from Bankstahl et al. [9] and Wagner et al. [30], respectively. Individual profiles from each animal or human were analyzed using the common data analysis approaches for PET (PK modeling of individual profiles) [33,34]. In both studies, a two-tissue-4-rate constant (2T4K) compartment model was applied to estimate the brain-to-plasma partition coefficient, referred to as the volume of distribution in PET literature ($V_{\text{T-2T4K}}$), and the rate constants describing exchange of radioactivity between the plasma and the two brain tissue compartments. To further obtain a model-independent estimate of the brain-to-plasma partition coefficient, Logan graphical analysis [34] was used ($V_{\text{T-Logan}}$). Data obtained during and immediately after tariquidar treatment, i.e., the last part of the baseline scans, were not included when estimating $V_{\text{T-2T4K}}$ and $V_{\text{T-Logan}}$.

Table 2 Number of human volunteers (*n*), weight at time of PET, injected doses (average ± standard deviation) of (*R*)-[^{11}C]verapamil for baseline, and post-inhibition scans after tariquidar (2 mg/kg) treatment

	Healthy volunteers and 2 mg/kg tariquidar treated
Number	5
Body weight (kg)	74±5
Baseline (*R*)-[^{11}C]verapamil (MBq)	379±11
I.V. injection time (sec)	51±10
Post-inhibition (*R*)-[^{11}C]verapamil (MBq)	389±15
I.V. injection time (sec)	43±11

NLME modeling

For modeling of the metabolite-corrected plasma and brain concentration-time curves during the entire scan period, NLME modeling in NONMEM VI (GloboMax LLC, Hanover, MD, USA) was applied in order to predict the rate constants describing the PK of (*R*)-[^{11}C]verapamil and the effects of tariquidar on (*R*)-[^{11}C]verapamil PK. Data from all subjects and all scans were analyzed simultaneously to yield population estimates of PK parameters as well as estimates of inter-animal variability. Covariate analysis allowed for the identification of the specific sources of variability. The subroutine ADVAN 9 and first-order conditional estimation with interaction were used throughout the modeling procedure. Model selection was based on the objective function value (OFV, the lowest value corresponds to the best model), model parameter uncertainty, and graphic analysis using Xpose 4 [35] implemented in software R 2.7.1. (The R Foundation for Statistical Computing). Outcome parameters were viewed and compared in Census [36]. For nested models, OFV reductions of 3.83, 6.63, and 10.83 units correspond to improved fits at $p < 0.05$, $p < 0.01$, and $p < 0.001$ levels. The inter-individual variation of the parameters was described by the exponential variance model:

$$\theta_i = \theta_{\text{pop}} * exp(\eta_i), \quad (1)$$

where θ_i is the parameter in the ith animal, θ_{pop} is the parameter in a typical animal, and η_i is the inter-animal

variability, which is assumed to be normally distributed around zero with a standard deviation ω, to distinguish the ith animal from the typical value as predicted from the regression model. Inter-animal variation was studied on all parameters and was included if the model was improved significantly (OFV > 3.83). To test the significance of the covariate inclusion, e.g., effect of tariquidar and SE, a stepwise forward addition and backward deletion approach was applied, and covariates were only kept in the model if they significantly improved the model. Finally, proportional error models were included for the residual variability, i.e., variability that remained unexplained after inclusion of inter-animal variability and covariates. More comprehensive description of NLME modeling can be found elsewhere, for example in the paper by Pillai et al. [37].

The model development was carried out using the rat dataset (WB region) and the model was built in sequential steps. The first step was to develop a PK model for (*R*)-[^{11}C]verapamil plasma concentration-time profiles. Two and three compartment models were evaluated. Treatment (tariquidar-treated or tariquidar-untreated) and rat group (control or 48-h post SE) were defined as covariates ($\mathrm{Eff}_{\mathrm{tariquidar}}$ and $\mathrm{Eff}_{\mathrm{SE}}$) and their effects on the parameter estimates were studied. Next, a PK model of (*R*)-[^{11}C]verapamil concentration-time profiles in brain was developed. Two and three compartment models were evaluated, and again treatment and rat group were defined as covariates. Finally, in the last step of the model development, the PK models for (*R*)-[^{11}C]verapamil kinetics in plasma and brain were merged.

The increased uptake of (*R*)-[^{11}C]verapamil into the brain after administration of tariquidar was assumed to be either due to increased transport of (*R*)-[^{11}C]verapamil into the brain (i.e., increased Q_{in}, Equation 2) or decreased transport of (*R*)-[^{11}C]verapamil out of the brain (i.e., decreased Q_{out}, Equation 3) [25].

$$\frac{dVER_{br1}}{dt} = D \cdot Q_{in} \cdot VER_c - Q_{out} \cdot VER_{br1} \quad (2)$$

$$\frac{dVER_{br1}}{dt} = Q_{in} \cdot VER_c - D \cdot Q_{out} \cdot VER_{br1} \quad (3)$$

$$\frac{dVER_{br2}}{dt} = Q_{br} \cdot VER_{br1} - Q_{br} \cdot VER_{br2}, \quad (4)$$

where $\mathrm{VER}_{\mathrm{br1}}$ and $\mathrm{VER}_{\mathrm{c}}$ are the (*R*)-[^{11}C]verapamil concentrations in the central brain compartment and in plasma, respectively, and D (Equations 2 and 3) describes the effect of tariquidar on the transport of (*R*)-[^{11}C]verapamil between plasma and brain. D was considered to affect the clearance out of the brain (Q_{out}) or the clearance into the brain (Q_{in}). Q_{br} is the bidirectional clearance between the central and the peripheral brain compartments (see also Figure 2). Different models for describing D were tested, including indirect effect models based on tariquidar plasma concentration or administered dose or as a combination of categorical covariates for tariquidar treatment and scan (see 'Results' section). A second (peripheral) brain compartment was evaluated for (*R*)-[^{11}C]verapamil, where $\mathrm{VER}_{\mathrm{br2}}$ is the (*R*)-[^{11}C]verapamil concentration in the peripheral slow equilibrating brain compartment (Equation 4). The final PK model developed for the WB region of the rat was then applied to the selected brain regions of interest (CS, EC, Shipp, THipp, Th, Cer, and FMC), respectively. To investigate whether the increase of (*R*)-[^{11}C]verapamil brain uptake during and after treatment with tariquidar (60 to 140 min of baseline scan) influenced the model outcome parameters, the final model was applied to the first 60 min of the baseline (i.e., excluding the data acquired during and immediately after tariquidar administration) and the post-inhibition scan only. The effect of tariquidar (D) was studied on the Q_{in} and the Q_{out} of (*R*)-[^{11}C]verapamil brain uptake. Additionally, the model was applied to the human data set,

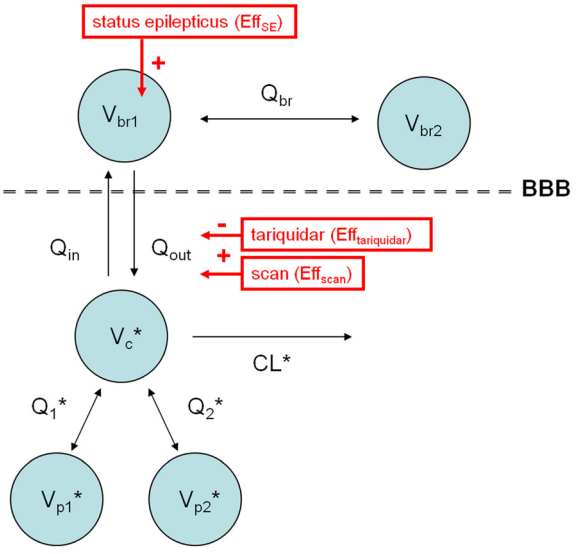

Figure 2 The final population model. V_c, V_{p1} and V_{p2} are the pharmacological volumes of distribution in central and two peripheral plasma compartments, while V_{br1} and V_{br2} are the volumes of distribution in central and peripheral brain compartments, respectively. CL, Q_1, Q_2, Q_{in}, Q_{out}, and Q_{br} are total body clearance, bidirectional clearance between plasma and peripheral compartment 1, bidirectional clearance between plasma and peripheral compartment 2, clearance into the brain, clearance out of the brain, and bidirectional clearance between central and peripheral brain compartments, respectively. Plus sign (+) indicates an increase in V_{br1} due to rat group ($\mathrm{Eff}_{\mathrm{SE}}$) and the effect of tariquidar ($\mathrm{Eff}_{\mathrm{tariquidar}}$), resulting in a decrease in Q_{out}. Asterisk (*) indicates the parameter estimates, which were fixed during modeling procedure, though V_{br2} was only fixed in rats.

and the influence of including or excluding (*R*)-[^{11}C]verapamil brain concentrations during and after the tariquidar administration (40 to 120 min of baseline scan) on the model outcome parameters was evaluated. Volume of distribution ($V_{T\text{-}NLME}$) was calculated as the ratio Q_{in}/Q_{out} and compared with $V_{T\text{-}2T4K}$ values obtained with standard PET PK modeling.

Statistics

Differences between groups were analyzed by 2-way ANOVA including Bonferroni correction using PRISM 5 software (GraphPad Software, La Jolla, CA). The level of statistical significance was set to $p < 0.05$.

Results

WB (*R*)-[^{11}C]verapamil time-activity curves expressed as SUV at baseline and in the post-inhibition scan are shown for naïve and 48-h post SE rats in Figure 3 and for humans in Figure 4. Both in rats and humans, tariquidar administration during the baseline scan resulted in an immediate rise in brain activity concentrations.

NLME modeling of plasma and brain PK with and without tariquidar administration

NLME modeling was used to study the kinetics of (*R*)-[^{11}C]verapamil in plasma and brain. Metabolite corrected plasma curves were best described with a three compartment model. Inclusion of covariates for describing the effect tariquidar treatment ($Eff_{tariquidar}$) and rat group (Eff_{SE}) did not result in a significant model improvement, when applied to any of the PK parameters of the plasma model and were, therefore, not included. Parameter estimates, the relative standard error (%), and the inter-animal variability for the plasma model are given in Table 3. Brain PK in both rats and humans was best described with a two-compartment model. The brain model was combined with the plasma PK model. For rats, plasma parameter estimates were fixed according to the best plasma model (see Table 3). In addition, the pharmacological volume of distribution of the peripheral brain compartment, V_{br2}, was fixed to a value of 2 ml, i.e. the total volume of a rat brain [38]. All other brain parameter estimates were allowed to freely change. For the human data, plasma parameters were also fixed, whereas the brain parameter estimates were allowed to freely change. The final model is shown in Figure 2, and the model diagnostics plots for the rat model are shown in Figure 5. Population parameter estimates of the (*R*)-[^{11}C]verapamil brain model for all studied brain regions of interest are shown in Table 4 for rats and humans. (*R*)-[^{11}C]verapamil concentration-time profiles in rats and model predictions of WB (data from 0 to 140 min and 180 to 240 min) and WB* (data from 0 to 60 min and 180 to 240 min) are shown in Figure 6. For the human data modeling, results of (*R*)-[^{11}C]verapamil concentration-time curves of the WB gray matter (data from 0 to 120 min and 240 to 280 min) and WB* gray matter (data from 0 to 40 min and 240 to 280 min) are shown in Figure 7. Structural model parameters were obtained for the clinical data (Table 3), but due to the relatively small sample size ($n = 5$), reliable estimates of inter-individual variation and standard deviations could not be obtained.

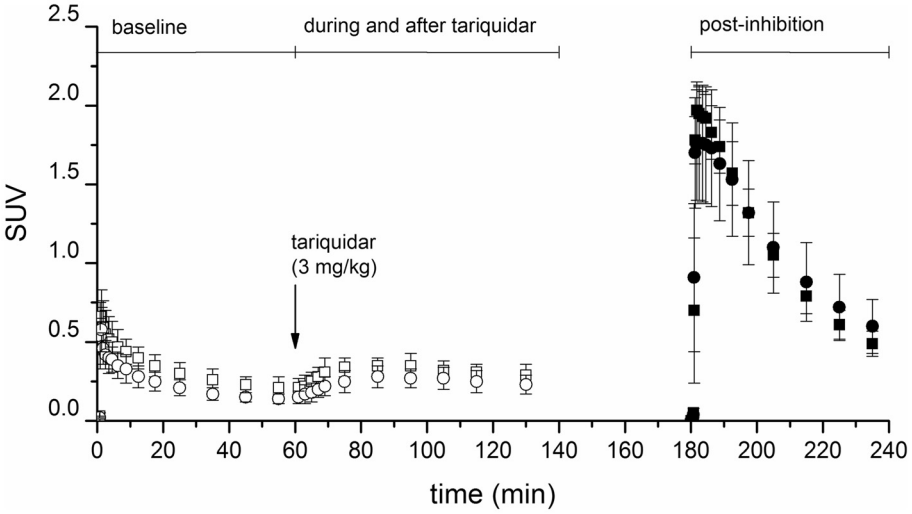

Figure 3 WB (*R*)-[^{11}C]verapamil time-activity curves in rats. Average ± standard deviation (*R*)-[^{11}C]verapamil concentration-time curves in rat WB expressed as SUV for naïve (squares) and 48-h post SE (circles) animals at baseline (open symbols) and at post-inhibition (full symbols). Tariquidar (3 mg/kg) was administered 60 min after the start of the baseline scan as an I.V. bolus over 60 sec (arrow).

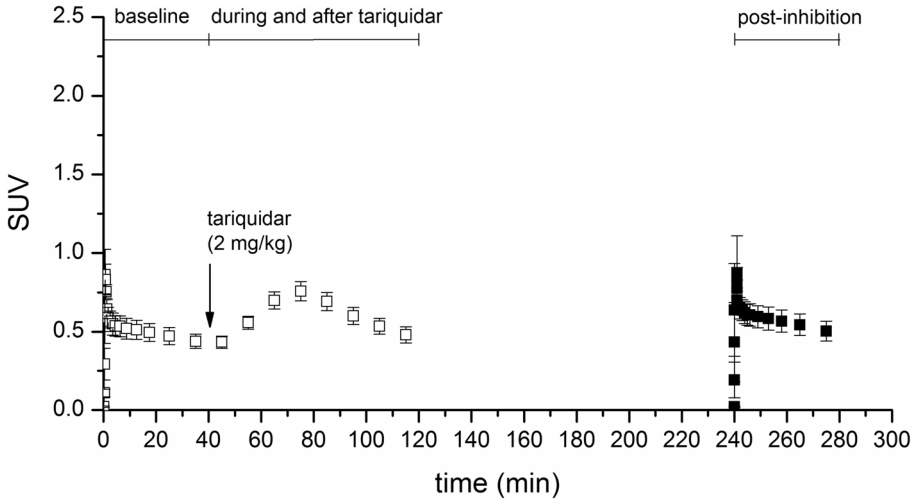

Figure 4 WB (*R*)-[^{11}C]verapamil time-activity curves in humans. Average ± standard deviation (*R*)-[^{11}C]verapamil concentration-time curves in human WB gray matter expressed as SUV at baseline (open symbols) and at post-inhibition (full symbols). Tariquidar (2 mg/kg) was administered 40 min after the start of the baseline scan as an infusion over 30 min (arrow).

Influence of tariquidar on (*R*)-[^{11}C]verapamil transport across the BBB

To investigate the mechanism of P-gp inhibition, tariquidar treatment was included as a covariate for the influx clearance from the plasma compartment into the first brain compartment (Q_{in}) or for the efflux clearance from the first brain compartment into the plasma compartment (Q_{out}). The effect (D) of tariquidar treatment was best described as a combination of two categorical covariates and was defined as:

$$D = \mathrm{Eff}_{\mathrm{tariquidar3}}{}^{(\mathrm{cov})} * \mathrm{Eff}_{\mathrm{scan}}{}^{(\mathrm{cov})}$$
$$\mathrm{cov} = 0 \; or \; 1 \tag{5a}$$

$$D = \mathrm{Eff}_{\mathrm{tariquidar15}}{}^{(\mathrm{cov})} * \mathrm{Eff}_{\mathrm{scan}}{}^{(\mathrm{cov})}$$
$$\mathrm{cov} = 0 \; or \; 1 \tag{5b}$$

$\mathrm{Eff}_{\mathrm{tariquidar3}}$ and $\mathrm{Eff}_{\mathrm{tariquidar15}}$ are the estimated effects of tariquidar for the 3 and 15 mg/kg doses, respectively. The exponent, cov, was assigned to a value of 0 when no tariquidar was administered or 1 when tariquidar was administered. $\mathrm{Eff}_{\mathrm{scan}}$ describes the difference in tariquidar effect between baseline and post-inhibition scans. The exponent, cov, of $\mathrm{Eff}_{\mathrm{scan}}$ was assigned to a value of 0 and 1 for the baseline and post inhibition scan, respectively. The total effect of tariquidar inhibition, D, was therefore the fractional change in transport caused by tariquidar while also taking into account changes of tariquidar-induced P-gp inhibition occurring between the two scans (baseline or post-inhibition) as it is likely that the inhibition is changing due to the elimination of tariquidar from the plasma and brain.

OFV was found to be lower when tariquidar treatment affected Q_{out} (Equation 3) compared when tariquidar treatment affected Q_{in} (Equation 2) in all studied brain regions. For example, in WB, the effect of tariquidar on Q_{out} yielded an OFV (the lowest value corresponds to the best model) of −1,676, while the effect of tariquidar

Table 3 Population parameter estimates and relative standard errors (%) of the (*R*)-[^{11}C]verapamil plasma model using mixed effects modeling of the WB region of interest of rats and humans

Pharmacokinetic parameters	Rat		Human estimates
	Estimates	Inter-animal variability	
Vc (ml)	38.8	0.162	2580
	(7.27)	(52.3)	(–)
V_{p1} (ml)	141	0.169	57900
	(17.6)	(23.3)	(–)
V_{p2} (ml)	1580	-	41100
	(17.6)		(–)
CL (ml·min^{-1})	16.4	0.162	538
	(10.3)	(52.3)	(–)
Q_1 (ml·min^{-1})	29.1	0.169	6550
	(7.77)	(23.3)	(–)
Q_2 (ml·min^{-1})	22.3	0.162	5880
	(10.0)	(52.3)	(–)
Residual error plasma	0.482	-	0.654
	(6.93)		(–)

For definition of parameters, please refer to the legend of Figure 2. The RSA are given in parentheses after the estimates.

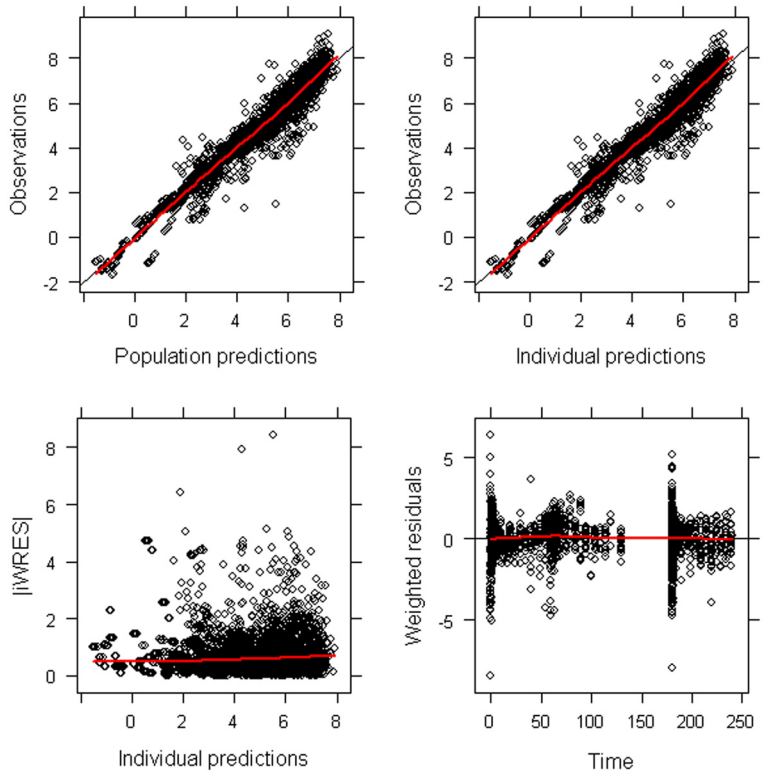

Figure 5 Diagnostic plots for the final population model including both brain and plasma (*R*)-[^{11}C]verapamil concentrations. Each individual data point is represented by one dot. The red line represents the average observation. Observations are plotted against population predictions (upper left panel) and individual predictions (upper right panel). Data points are randomly distributed along the line of identity, indicating that the concentrations are adequately described by the model. Absolute individual weighted residuals versus individual predictions (lower left panel) and weighted residuals versus time (lower right panel) are plotted. Most residuals are clustered around zero, while there are outliers at early time points.

on Q_{in} resulted in an OFV of −1,541. Afterwards, the model was applied to the dataset, excluding data acquired during and after tariquidar administration. Again, the OFV was lower in all regions when the tariquidar effect was applied on Q_{out} compared to Q_{in}. Parameter estimates, when including or excluding the data acquired during and immediately after tariquidar administration, were in general comparable. The parameter estimates for the whole brain regions when including (WB) and excluding (WB*) this data are given in Table 4. In Figure 8E, Q_{in} and Q_{out} values for baseline scans in rats are shown. At baseline, statistically significant differences between Q_{in} and Q_{out} were observed for all brain regions in rats, except for FMC. In all outlined brain regions Q_{out} was higher than Q_{in}, while in WB, Q_{in} was higher than Q_{out}. Additionally, in all brain regions, Q_{out} was decreased during and after tariquidar administration as compared with baseline scans (Figure 8F). Mean decrease in Q_{out} relative to baseline scan was −84±5% for 3 mg/kg and −86±4% for 15 mg/kg tariquidar. For the 3 mg/kg tariquidar group, largest decreases of Q_{out} relative to baseline scan were found for CS (−89%, $Eff_{tariquidar}$ = 0.11) followed by SHipp (−88%, $Eff_{tariquidar}$ = 0.12) and Th (−88%, $Eff_{tariquidar}$ = 0.12), and smallest decreases were found for Cer and EC (both −77%, $Eff_{tariquidar}$ = 0.23) (Table 4). For the 15 mg/kg tariquidar group, largest decreases in Q_{out} were found in CS, SHipp, and Th (all −90%, $Eff_{tariquidar}$ = 0.10), and smallest decreases were found in EC (−79%, $Eff_{tariquidar}$ = 0.215) (Table 4). In summary, there was a trend that Q_{out} was further reduced in 15 mg/kg as compared with 3 mg/kg tariquidar treated animals in all regions (Figure 8F). However, the difference in Q_{out} between 3 and the 15 mg/kg treated animals was statistically significant only in Cer. Also when comparing Q_{out} estimated when data during and immediately after tariquidar administration was excluded, Cer was the only region in which Q_{out} differed between 3 and the 15 mg/kg treated animals (Figure 8G). When excluding the data during and immediately after tariquidar administration, mean decrease of Q_{out} relative to baseline scans was −78±7% for 3 mg/kg and −82±6% for 15 mg/kg tariquidar (Figure 8G). Thus, Q_{out} was

Table 4 Population parameter estimates and relative standard errors (%) of (*R*)-[^{11}C]verapamil brain model are shown for all investigated brain regions

	Species										
	Rat									Human	
Brain region	WB^{*,a}	WB^{b}	CS	EC	SHipp	THipp	Th	Cer	FMC	WB^{*,a}	WB^{b}
OFV	−604	−1676	−1420	−1652	−1500	−954	−1559	−1562	−1365	7799	−357
Model parameters											
V_{br1} (ml)	0.132	0.132	0.119	0.155	0.151	0.129	0.156	0.192	0.088	2.29	3.17
	(10.5)	(11.3)	(10)	(11.4)	(9.74)	(27.2)	(12.2)	(19.2)	(15.8)	(–)	(–)
V_{br2} (ml)	2	2	2	2	2	2	2	2	2	13.0	18.4
	(–)	(–)	(–)	(–)	(–)	(–)	(–)	(–)	(–)	(–)	(–)
Q_{in} (ml·min^{-1})	5.48	5.62	2.05	3.32	2.49	1.98	2.43	2.44	1.79	713	588
	(13.0)	(12.5)	(12.8)	(16.8)	(12.7)	(24.5)	(11.3)	(14.2)	(19.2)	(–)	(–)
Q_{out} (ml·min^{-1})	3.56	3.60	3.45	3.91	4.56	2.99	4.39	3.01	1.97	1410	1080
	(12.6)	(12.5)	(12.5)	(16.3)	(12.5)	(21.8)	(11.3)	(13.9)	(19.1)	(–)	(–)
Q_{br} (ml·min^{-1})	0.115	0.115	0.114	0.111	0.113	0.108	0.129	0.118	0.12	1.26	1.71
	(3.2)	(3.05)	(3.43)	(3.71)	(3.87)	(4.63)	(3.45)	(3.24)	(3.58)	(–)	(–)
Residual error brain	0.404	0.382	0.44	0.387	0.421	0.571	0.016	0.407	0.454	0.295	0.27
	(5.1)	(4.61)	(5.3)	(6.25)	(4.18)	(14.4)	(3.93)	(5.72)	(6.32)	(–)	(–)
Covariates											
Effect of pilocarpine induced SE											
Eff$^{c}_{SE}$	1.84	1.84	1.88	1.73	1.86	2.21	1.77	0.924	2.3	(–)	(–)
	(10.4)	(11.7)	(13.8)	(13.5)	(13.2)	(24.7)	(12.9)	(20.5)	(15.8)		
Effect of tariquidar											
Eff$_{tariquidar}$ (3 mg/kg or 2 mg/kg)^{d}	0.219	0.161	0.114	0.233	0.119	0.15	0.12	0.226	0.194	0.993	0.483
	(5.84)	(4.16)	(3.89)	(5.54)	(5.49)	(5.51)	(5.33)	(5.31)	(4.42)	(–)	(–)
Eff$_{tariquidar}$ (15 mg/kg)^{d}	0.168	0.135	0.101	0.215	0.101	0.134	0.103	0.148	0.155	(–)	(–)
	(5.22)	(6.94)	(7.71)	(6.56)	(9.3)	(7.61)	(9.01)	(8.65)	(7.74)	-	-
Effect of scan on tariquidar induced P-gp inhibition											
Eff$^{d}_{scan}$	(–)	1.33	1.29	1.37	1.29	1.25	1.21	1.52	1.4	(–)	2.28
	-	(5.67)	(6.78)	(5.47)	(7.1)	(6.21)	(6.08)	(6.97)	(6.06)	-	(–)

All (*R*)-[^{11}C]verapamil plasma model parameter estimates outlined in Figure 2, obtained from final plasma model were fixed and the parameter estimate for the second brain compartment V_{br2} was fixed in rats to 2 ml. Parameters are given for the whole brain excluding (WB*) and including (WB) the increase of (*R*)-[^{11}C] verapamil brain uptake during and after treatment with tariquidar, corpus striatum (CS), entorhinal cortex (EC), septal hippocampus (SHipp), temporal hippocampus (THipp), thalamus (TH), cerebellum (Cer), and frontal motor cortex (FMC) for rat; WB* and WB for human. [a]WB* is the whole brain region excluding data from 60 to 140 min rat or 40 to 120 min human (baseline and post-inhibition scan are considered, as used for kinetic modeling). [b]WB is the whole brain region including data from 60 to 140 min rat or 40 to 120 min human (baseline, during, and after tariquidar, and post-inhibition scan are considered). [c]Eff$_{SE}$ was a significant covariate on V_{br1}. [d]The effect of tariquidar, Eff$_{tariquidar}$, is on Q_{out} the efflux clearance from the central brain compartment to the plasma compartment, while Eff$_{scan}$ also takes into account changes occurring between scans (baseline or post-inhibition).

less decreased relative to baseline scans in the post-inhibition scan as compared to the last part of the first scan when tariquidar had been administered (comparison between Figure 8F and Figure 8G). In humans, Q_{out} was 1.8-fold higher than Q_{in} in the baseline scan (Figure 8D). Q_{out} during and after tariquidar administration was decreased by −52% compared with Q_{out} at baseline (Eff$_{tariquidar}$ = 0.48) (Figure 8H, Table 4). During the post-inhibition scan, Q_{out} was completely restored to its baseline value (Eff$_{tariquidar}$ = 0.99).

Volume of distribution ($V_{T\text{-}NLME}$)

$V_{T\text{-}NLME}$ (Q_{in}/Q_{out}) values at baseline and after tariquidar administration are shown in Figure 8A,B,C,D for rats and humans. Tariquidar increased $V_{T\text{-}NLME}$ by approximately 6.2-fold after 3 mg/kg dose and 7.4-fold after 15 mg/kg dose in the whole brain region when all data were analyzed (Figure 8C). $V_{T\text{-}NLME}$ increase was lowest in EC (fourfold) and highest in CS (ninefold) for the 3 mg/kg tariquidar treated group. Also, for the 15 mg/kg tariquidar group, $V_{T\text{-}NLME}$ increase was lowest in EC (fivefold)

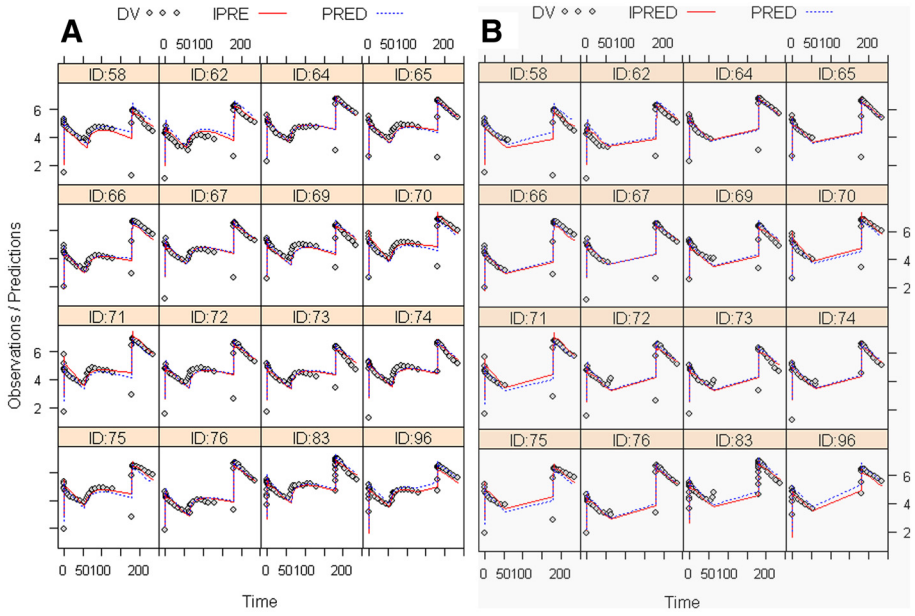

Figure 6 Modeling results of (*R*)-[^{11}C]verapamil concentration-time curves in WB of rats in ln(Bq/ml) over time (min). (**A**) WB was compared with (**B**) WB* excluding the increase of (*R*)-[^{11}C]verapamil brain uptake after treatment with tariquidar from 60 to 140 min. Tariquidar (3 or 15 mg/kg) was administered at 60 min after start of tracer injection as an I.V. bolus over 60 sec and the post-inhibition scan was started 2 h after tariquidar administration. Each panel represents one animal (not all 21 are shown), open gray circles represent measurements (DV), solid red lines represent the model predictions for individual rats (IPRE), and broken blue lines represent the population model predictions (PRED).

and highest in CS (tenfold). $V_{\text{T-NLME}}$ was slightly decreased when the data acquired during and immediately after tariquidar administration (scan 1, 60 to 140 min) was excluded. This was the result of a slightly decreased $\text{Eff}_{\text{tariquidar}}$ in the second scan compared to the first scan. In humans, a twofold increase in $V_{\text{T-NLME}}$ relative to baseline was observed during and after tariquidar administration (Figure 8D). In contrast, $V_{\text{T-NLME}}$ was unchanged in the post-inhibition scan as compared with baseline (Figure 8D).

The influence of rat group (status epilepticus)

The model was improved when Eff_{SE} was included as a covariate for the volume of distribution of the central brain compartment V_{br1}:

$$V_{\text{br1,ind}} = V_{\text{br1,pop}} * \text{Eff}_{\text{SE}}{}^{(\text{cov})} \qquad \text{cov} = 0 \textit{ or } 1, \quad (6)$$

where Eff_{SE} is the estimated influence of pilocarpine-induced SE on V_{br1} (Equation 6) and implies a fractional difference between control and 48-h post SE rats. Hence,

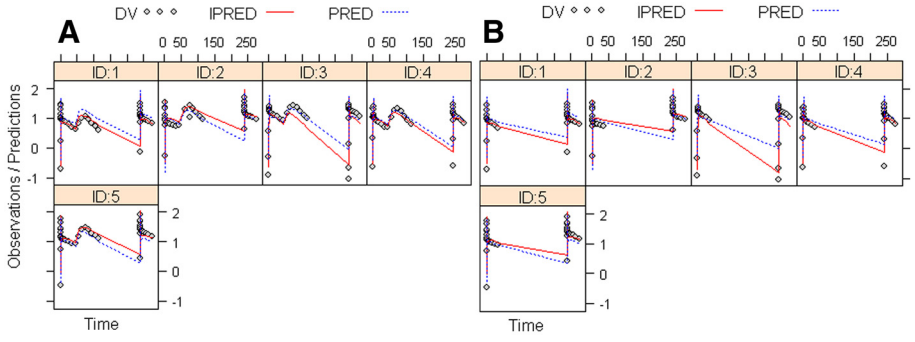

Figure 7 Modeling results of (*R*)-[^{11}C]verapamil concentration-time curves in WB gray matter in ln(Bq/ml) over time (min). (**A**) WB gray matter was compared with (**B**) WB* gray matter excluding the increase of (*R*)-[^{11}C]verapamil brain uptake after treatment with tariquidar. Tariquidar (2 mg/kg) was administered at 40 min after start of tracer injection as an intravenous infusion over 30 min and post-inhibition scan was started 2 h 50 min after end of tariquidar infusion. Each panel represents one volunteer, open gray circles represent measurements (DV), solid red lines represent the model predictions for each individual subject (IPRE), and broken blue lines represent the population model predictions (PRED).

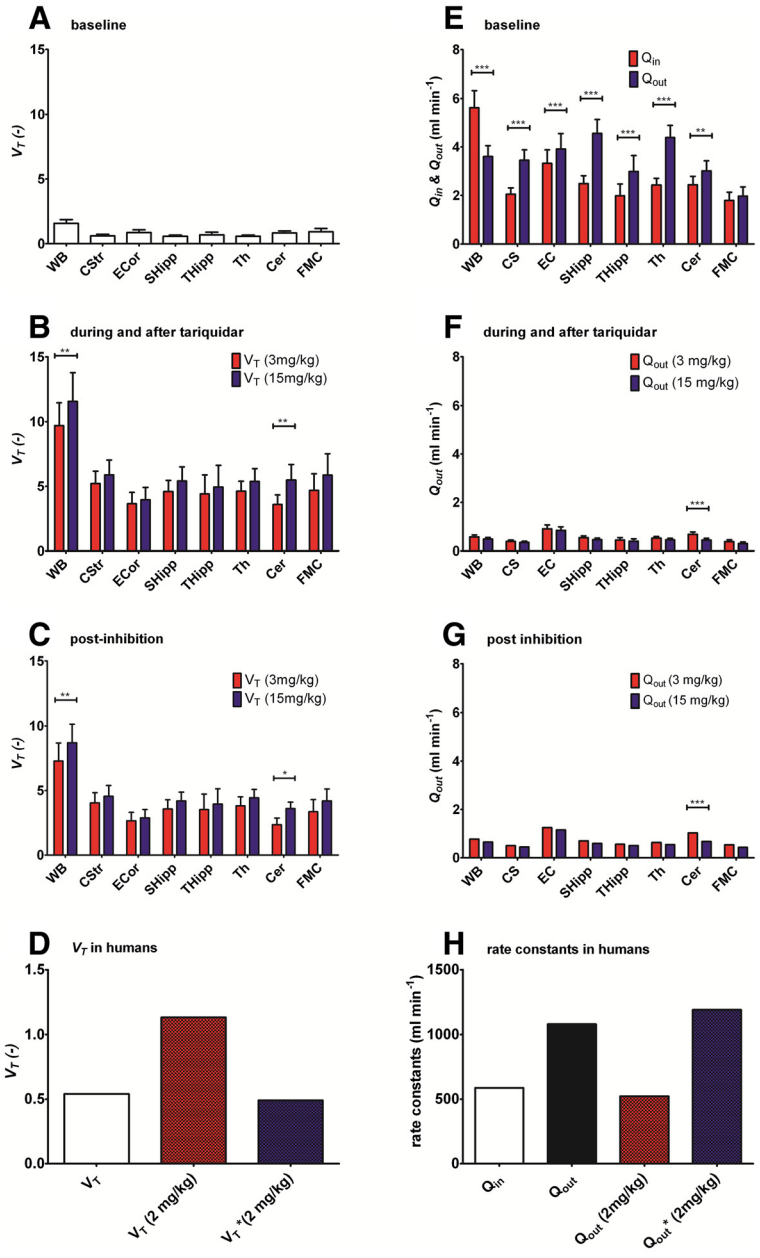

Figure 8 Brain-to-plasma partition coefficients (A-D) and transport clearances across the BBB (E-H). (**A**) $V_{T\text{-NLME}}$ in rats at baseline, (**B**) $V_{T\text{-NLME}}$ in rats during and after tariquidar administration, (**C**) $V_{T\text{-NLME}}$ in rats in post-inhibition scan, and (**D**) $V_{T\text{-NLME}}$ in WB in humans at baseline (V_T), during and after tariquidar administration (V_T (2 mg/kg)) and in post-inhibition scan (V_T^*(2 mg/kg)). (**E**) Q_{in} and Q_{out} in rats at baseline, (**F**) Q_{out} in rats during and after tariquidar administration (3 or 15 mg/kg), (**G**) Q_{out} in rats in post-inhibition scan, and (**H**) Q_{in}, Q_{out} at baseline, Q_{out} during and after tariquidar administration (2 mg/kg), and Q_{out}^* in post-inhibition scan (2 mg/kg) in humans. *$p < 0.05$, **$p < 0.01$, ***$p < 0.001$; not significant $p > 0.05$.

the exponent, cov, in Equation 6 was assigned to a value of 0 for the control rat group, while it was assigned to a value of 1 for the 48-h post SE group.

Eff_{SE} was found to be a significant covariate that increased V_{br1} in 48-h post SE rats as compared with control rats (see Figure 2, Table 4) in all brain regions except Cer. The largest increase in V_{br1} in the 48-h post SE group was observed for FMC (+130%, Eff_{SE} = 2.3) and in THipp (+121%, Eff_{SE}= 2.21) (Table 4). In Cer, a small decrease in V_{br1} for 48-h post SE rats as compared with naïve rats was found (−8%, Eff_{SE} = 0.92). Eff_{SE} was not considered for the analysis of the human data set due to the fact that only healthy subjects participated in the clinical study.

Discussion

In the present study, we used NLME modeling to study the PK of (*R*)-[^{11}C]verapamil in plasma and brain, and the influence of tariquidar on (*R*)-[^{11}C]verapamil brain PK to gain better insight into the mechanism of P-gp modulation by tariquidar. Moreover, our goal was to evaluate if the increase in brain activity induced by tariquidar during the first PET scan is better suited to describe regional and species differences and differences between control and post SE rats in cerebral P-gp function/expression as compared with using data from the post-inhibition scan alone. The developed model described the rat data well (Figure 6) and was then used to model the clinical data set. The small number of human subjects made it difficult to obtain estimates of the inter-individual variation in the human data set, but the model converged and, although the fit was not perfect, provided estimates of all structural model parameters. However, the variation in the human PK data set between the five subjects was rather large, and in combination with the few subjects, the results should be interpreted with some caution.

During model development we tested certain indirect response models [39] as used by Syvänen et al. [25], which either incorporate tariquidar plasma concentration or administered dose to describe the effect of tariquidar on (*R*)–[^{11}C]verapamil exchange between plasma and brain. These models described (*R*)–[^{11}C]verapamil kinetics well, but were not able to estimate the half maximum effect dose (ED_{50}) of tariquidar for P-gp inhibition properly as our study only contained two dose groups (3 and 15 mg/kg tariquidar). Thus, a simplified model describing the effect of tariquidar as a categorical covariate was used. The decline in effect of tariquidar between the two scans, due to tariquidar elimination, was accounted for by a second categorical covariate (Eff_{scan}). The appropriateness of the model was confirmed as $Eff_{tariquidar}$*Eff_{scan} when including all data equaled $Eff_{tariquidar}$ when omitting data during and immediately after tariquidar administration. We defined the NLME model in terms of clearances (ml/min) between model compartments and volumes of distribution (ml) as this is standard in conventional PK analysis. To compare different modeling approaches, we calculated V_T values from the outcome parameters obtained with NLME modeling ($V_{T\text{-}NLME}$ as the ratio Q_{in}/Q_{out}) and compared them with the respective $V_{T\text{-}2T4K}$ values obtained with standard PK modeling [9,30]. Overall, $V_{T\text{-}2T4K}$ obtained with PET PK modeling and $V_{T\text{-}NLME}$ obtained with NLME modeling were comparable. Tariquidar decreased the parameter Q_{out} which led to an increase in $V_{T\text{-}NLME}$. This is in line with previous publications using standard PET PK modeling approaches, although the extent of the increase is somewhat larger in the present study as data during and immediately after the tariquidar administration were included (Table 5). This shows that excluding data during and immediately after P-gp inhibition leads to an underestimation of the effect of P-gp inhibition on brain concentrations of P-gp substrates. After P-gp inhibition in humans, $V_{T\text{-}2T4K}$ was slightly increased, while a decrease was observed for $V_{T\text{-}NLME}$. This is likely due to the fact that, in the standard PET approach, one subject is driving the average, while with NLME modeling, the model is

Table 5 Comparison of volumes of distribution (V_T) values of naïve, 48-h SE rats, and humans obtained with Logan analysis, PK modeling, and nonlinear mixed effects modeling, respectively

Sample	Logan analysis[a]		PK modeling[a] (2T4K)		Nonlinear mixed effects modeling		
	WB*	Cer	WB*	Cer	WB*	WB	Cer
Control rats							
Baseline	1.6 (16)	2.0 (19)	1.8 (16)	2.2 (18)	1.5 (18)	1.6 (18)	0.81 (20)
Post-inhibition	7.6 (13)	6.1 (9)	7.8 (14)	6.1 (9)	7.0 (19)	9.6 (18)	2.4 (21)
Increase after 3 mg/kg tariquidar[b]	4.8-fold	3.1-fold	4.4-fold	2.8-fold	4.6-fold	6.2-fold	4.4-fold
48-h post SE rats							
Baseline	1.4 (8)	1.3 (7)	1.5 (12)	1.5 (6)	1.5	1.6	0.81
Post-inhibition	7.4 (11)	3.5 (13)	7.6 (12)	3.6 (14)	7.0	9.6	2.4
Increase after 3 mg/kg tariquidar[b]	5.5-fold	2.6-fold	5.1-fold	2.4-fold	4.6-fold	6.2-fold	4.4-fold
Human							
Baseline scan	0.64 (1)		0.65 (6)	-	0.54 (–)	0.51 (–)	-
Post-inhibition	0.79 (1)		0.80 (2)	-	0.49 (–)	0.79 (–)	-
Increase after 2 mg/kg tariquidar[b]	1.2-fold		1.2-fold	-	No difference	1.5-fold	-

V_T values were expressed as average and relative standard errors (%) for the WB region and Cer at baseline and post-inhibition scan. [a]Logan and 2T4K results were obtained from Bankstahl et al. [9] for rats and from Wagner et al. [30] for humans. [b]Increase after tariquidar administration for NLME modeling is based on the estimated covariate effect $Eff_{tariquidar}(1/Eff_{tariquidar})$.

less sensitive to one subject as all data are analyzed simultaneously.

The major findings of this study are as follows: First, it has been debated whether inhibition of P-gp affects the transport of substrates across the BBB into the brain (K_1, Q_{in}) or the transport out of the brain (k_2, Q_{out}). Two models have been suggested, i.e., influx hindrance and efflux enhancement. Influx hindrance can be described by the 'gatekeeper' model, where substrates are transported back from the lipid layers of the luminal cell membrane into the blood before they reach the cytoplasm. Efflux enhancement can be described by the 'vacuum cleaner' model [40] which suggests that substrates can be transported from the endothelial cells or brain parenchyma back into the blood. Thus, the question remains if tariquidar enhances brain distribution of (*R*)-[^{11}C]verapamil by increasing the influx (K_1, Q_{in}) or decreasing the efflux (k_2, Q_{out}) of the tracer. Our model clearly indicated that tariquidar enhances brain uptake of (*R*)-[^{11}C]verapamil by decreasing Q_{out} of the radiotracer. P-gp inhibition led to an on average sevenfold reduction in Q_{out} in rats (3 mg/kg tariquidar), while in humans (2 mg/kg tariquidar) a twofold reduction in Q_{out} was observed when all data were included into the model. When data during and immediately after tariquidar administration were excluded, an average fivefold reduction in Q_{out} was observed in rats. Thus, the reduction in Q_{out} when including the data obtained during and after tariquidar administration was more pronounced than when this part was excluded. This indicates that the effect of tariquidar on P-gp function is already declining at 2 h after tariquidar administration. In humans, the tariquidar effect on Q_{out} was apparent only during and after tariquidar administration and had completely disappeared in the post-inhibition scan. This highlights the importance of designing appropriate study protocols when investigating active transporters at the BBB as the onset and decline of inhibition is very rapid. Also, important to point out is that the analysis showed that Q_{out} and Q_{in} estimates were very similar regardless of whether the data from the tariquidar administration period were included or not, i.e., this confirms that the model is reliable and that only parameters that are expected to vary over time, e.g. the effect of tariquidar, are indeed changing.

Second, the study also indicated some regional and species differences in P-gp inhibition; large tariquidar-induced decreases in Q_{out} (CS, Th, and Hipp) indicated strongly enhanced brain uptake of (*R*)-[^{11}C]verapamil, while small decreases in Q_{out} (Cer, EC) indicated a weak enhancement in brain uptake of (*R*)-[^{11}C]verapamil as compared with baseline scans (Figure 8). A decrease in Q_{out} leads to an increased $V_{T\text{-}NLME}$ as $V_{T\text{-}NLME}$ is defined as the ratio between Q_{in} and Q_{out}. Thus, the developed NLME model indicated that, after P-gp inhibition, $V_{T\text{-}NLME}$ was significantly increased both in naïve and 48-h post SE rats. Inhibition with 3 mg/kg tariquidar resulted in regionally different enhancement of brain activity distribution, with weakest enhancement (low $V_{T\text{-}NLME}$) in Cer and strongest enhancement (high $V_{T\text{-}NLME}$) in CS and Th, similar to the findings of Kuntner et al. [10], who reported lowest $V_{T\text{-}2T4K}$ increases in Cer and highest $V_{T\text{-}2T4K}$ increases in Th of naïve rats after administration of 3 mg/kg tariquidar. (*R*)-[^{11}C]verapamil WB $V_{T\text{-}NLME}$ was about threefold lower at baseline in humans than in rats (0.51 vs. 1.6±0.3) (Table 5). This is also in good agreement with findings from Bauer et al. [18] reporting twofold lower $V_{T\text{-}2T4K}$ values in humans than in rats (Table 5). These observed differences could be due to different expression and transport capacity of P-gp.

Third, SE (Eff_{SE}) was found to increase V_{br1} in most regions leading to an increase in brain exposure time of (*R*)-[^{11}C]verapamil in 48-h post SE rats compared with controls. This is mainly because an increase in V_{br1} indicates increased distribution of (*R*)-[^{11}C]verapamil to the slow equilibrating brain compartment (V_{br2}). This in turn will slow down the elimination of (*R*)-[^{11}C]verapamil from the brain. The difference between the two groups was largest in FMC (Eff_{SE} = 2.3, Table 4). This is in line with results reported by Syvänen et al. [26], which showed that V_{br1} in WB was increased 1.3-fold in kainate-induced post SE rats. In contrast to all other regions, exposure time was decreased in Cer in 48-h post SE rats compared with controls (Eff_{SE} = 0.924, Table 4). In line with these findings, Bankstahl et al. reported an increase of $V_{T\text{-}2T4K}$ in FMC, while Cer showed the largest decrease of $V_{T\text{-}2T4K}$ in 48-h post SE rats compared with controls [9]. The decrease in $V_{T\text{-}2T4K}$ in Cer of 48-h post SE rats was presumably caused by a twofold upregulation of P-gp as compared with control rats as revealed by post-mortem immunohistochemical analysis of the brain tissue [9]. Opposite to the findings presented in this paper, Bankstahl et al. also reported decreases or non-significant differences between controls and 48-h post SE rats in CS, Hipp, and Th. However, when ranking the regional SE-induced differences reported in the present study and by Bankstahl et al., the order is the same: FMC > CS > Hipp > Th > Cer. Bankstahl et al. found these regional differences only after partial inhibition of P-gp with 3 mg/kg. In the present study, all data were analyzed simultaneously including data from rats administered with 3 and 15 mg/kg tariquidar. This may, at least in part, be a reason for the differences in magnitude of regional differences between the present study and the study by Bankstahl et al. The present study showed that the effect of SE was mainly influencing the distribution of (*R*)-[^{11}C]verapamil

within the brain (V_{br1}) and not the actual transport across the BBB (Q_{in}, Q_{out}). It was possible to make this distinction by parameterization of the model using distribution volumes (the pharmacological term) and clearances instead of rate constants which depend on distribution volumes and clearances. Again, the effect of SE was the same when including and excluding data from the tariquidar administration period which indicated that the model parameter estimates are robust and do not change when adding or deleting some of the data set.

Conclusion

This study showed that tariquidar enhances brain uptake of (*R*)-[^{11}C]verapamil by decreasing the outflux (Q_{out}) of the tracer across the BBB. Pilocarpine-induced SE did not directly influence (*R*)-[^{11}C]verapamil transport across the BBB but had an indirect influence on the (*R*)-[^{11}C]verapamil exposure time in brain by influencing the pharmacological volume of distribution in the brain (V_{br1}). For the quantitative analysis of PET data, the NLME modeling approach used in this study is an interesting supplemental tool to standard PET PK modeling approaches on individual level to increase mechanistic knowledge of radiotracer transport across the BBB.

Abbreviations

2T4K: Two tissue compartment model; BBB: Blood–brain barrier; Cer: Cerebellum region; CL: Systemic clearance; CS: Corpus striatum region; EC: Entorhinal cortex region; Eff_{scan}: Effect of scan 2 as a fractional change from scan 1; Eff_{SE}: Effect of pilocarpine-induced SE as a fractional change from control; $Eff_{tariquidar}$: Effect of tariquidar treatment as a fractional change from no treatment; FMC: Frontal motor cortex region; NLME: Nonlinear mixed effects; OFV: Objective function value; PD: Pharmacodynamics; PET: Positron emission tomography; P-gp: P-glycoprotein; PK: Pharmacokinetics; Q_1: Clearance from central compartment to first peripheral compartment; Q_2: Clearance from central compartment to second peripheral compartment; Q_{in}: Clearance from plasma to brain; Q_{out}: Clearance from brain to plasma; SE: Status epilepticus; Shipp: Septal hippocampus region; SUV: Standardized uptake value; Th: Thalamus region; THipp: Temporal hippocampus region; V_{br1}: Pharmacological distribution volume in first brain compartment; V_{br2}: Pharmacological distribution volume in second brain compartment; V_c: Pharmacological distribution volume in central compartment; V_{p1}: Pharmacological distribution volume in first peripheral compartment; V_{p2}: Pharmacological distribution volume in second peripheral compartment; $V_{T\text{-}Logan}$: The brain-to-plasma partition coefficient obtained with Logan analysis; $V_{T\text{-}NLME}$: The brain-to-plasma partition coefficient obtained with NLME; $V_{T\text{-}2T4K}$: The brain-to-plasma partition coefficient obtained with 2T4K; WB: Whole brain region.

Competing interests

The authors declare that they have no competing interests.

Authors' contributions

JM is the main author of the manuscript and performed all NLME modeling. CK performed the 2T4K modeling of the preclinical data and contributed to the interpretation of data. MB performed the human study including data acquisition and modeling. JPB contributed to the conception and design of the study, and acquired the preclinical data. MM and RAV contributed to the interpretation of data and drafting of the manuscript. OL contributed to the conception and design of the study, and was also involved in drafting the manuscript. SS contributed to the development of the NLME model and to the drafting of the manuscript. All authors read and approved the final manuscript.

Authors' information

JM is a post-graduate student developing new methods for analyzing PET data. CK, SS, and JPB are senior researchers focusing on preclinical and translational PET including pharmacokinetic modeling. MB is a senior researcher focusing on clinical PET. Professor RAV is an expert on animal models in epilepsy research. Professor MM is an expert in clinical pharmacology, and Professor OL specializes in the development of radiotracers for the imaging of CNS targets.

Acknowledgements

The authors thank Johann Stanek, Thomas Wanek, Thomas Filip, and Maria Zsebedics (Austrian Institute of Technology GmbH), and Marion Bankstahl (University for Veterinary Medicine, Hannover, Germany) for their skillful assistance during the performance of this study as well as the staff of the radiochemistry laboratory (Seibersdorf Laboratories GmbH) for their continuous support. This work was supported by funding from the European Community's Seventh Framework Programme (FP7/2007-2013) under grant agreement number 201380 ('Euripides') and from the Austrian Science Fund (FWF) project 'Transmembrane Transporters in Health and Disease' (SFB F35).

Author details

[1]Biomedical Systems, Health & Environment Department, AIT Austrian Institute of Technology GmbH, Seibersdorf 2444, Austria. [2]Department of Clinical Pharmacology, Medical University of Vienna, Währinger Gürtel 18-20, Vienna 1090, Austria. [3]Department of Nuclear Medicine, Hannover Medical School, Carl-Neuberg-Straße 1, Hannover 30625, Germany. [4]Epilepsy Institutes of The Netherlands Foundation, Achterweg 5, Heemstede 2103 SW, The Netherlands. [5]Division of Pharmacology, Leiden University, Einsteinweg 55, Leiden 2333 CC, The Netherlands. [6]Department of Public Health and Caring Sciences, Uppsala University, Rudbecklaboratoriet, Uppsala 751 85, Sweden.

Received: 30 August 2012 Accepted: 26 September 2012
Published: 16 October 2012

References

1. Kwan P, Brodie MJ: **Refractory epilepsy: mechanisms and solutions.** *Expert Rev Neurother* 2006, **6**(3):397–406.
2. Löscher W, Potschka H: **Drug resistance in brain diseases and the role of drug efflux transporters.** *Nat Rev Neurosci* 2005, **6**(8):591–602.
3. Kannan P, John C, Zoghbi SS, Halldin C, Gottesman MM, Innis RB, Hall MD: **Imaging the function of P-glycoprotein with radiotracers: pharmacokinetics and in vivo applications.** *Clin Pharmacol Ther* 2009, **86**(4):368–377.
4. Luurtsema G, Molthoff CF, Schuit RC, Windhorst AD, Lammertsma AA, Franssen EJ: **Evaluation of (R)-[11C]verapamil as PET tracer of P-glycoprotein function in the blood–brain barrier: kinetics and metabolism in the rat.** *Nucl Med Biol* 2005, **32**(1):87–93.
5. Mairinger S, Erker T, Müller M, Langer O: **PET and SPECT radiotracers to assess function and expression of ABC transporters in vivo.** *Curr Drug Metab* 2011, **12**(8):774–792.
6. Hendrikse NH, de Vries EG, Eriks-Fluks L, van der Graaf WT, Hospers GA, Willemsen AT, Vaalburg W, Franssen EJ: **A new in vivo method to study P-glycoprotein transport in tumors and the blood–brain barrier.** *Cancer Res* 1999, **59**(10):2411–2416.
7. Luurtsema G, Verbeek GL, Lubberink M, Lammertsma AA, Dierckx R, Elsinga P, Windhorst AD, van Waarde A: **Carbon-11 labeled tracers for in vivo imaging P-glycoprotein function: kinetics, advantages and disadvantages.** *Curr Top Med Chem* 2010, **10**(17):1820–1833.
8. Syvänen S, Hammarlund-Udenaes M: **Using PET studies of P-gp function to elucidate mechanisms underlying the disposition of drugs.** *Curr Top Med Chem* 2010, **10**(17):1799–1809.
9. Bankstahl JP, Bankstahl M, Kuntner C, Stanek J, Wanek T, Meier M, Ding XQ, Müller M, Langer O, Löscher W: **A novel positron emission tomography imaging protocol identifies seizure-induced regional overactivity of P-glycoprotein at the blood–brain barrier.** *J Neurosci* 2011, **31**(24):8803–8811.
10. Kuntner C, Bankstahl JP, Bankstahl M, Stanek J, Wanek T, Stundner G, Karch R, Brauner R, Meier M, Ding X, Müller M, Löscher W, Langer O: **Dose–response assessment of tariquidar and elacridar and regional**

quantification of P-glycoprotein inhibition at the rat blood–brain barrier using (R)-[(11)C]verapamil PET. *Eur J Nucl Med Mol Imaging* 2010, **37**(5):942–953.
11. Bankstahl JP, Löscher W: **Resistance to antiepileptic drugs and expression of P-glycoprotein in two rat models of status epilepticus.** *Epilepsy Res* 2008, **82**(1):70–85.
12. Dombrowski SM, Desai SY, Marroni M, Cucullo L, Goodrich K, Bingaman W, Mayberg MR, Bengez L, Janigro D: **Overexpression of multiple drug resistance genes in endothelial cells from patients with refractory epilepsy.** *Epilepsia* 2001, **42**(12):1501–1506.
13. Löscher W, Potschka H: **Role of multidrug transporters in pharmacoresistance to antiepileptic drugs.** *J Pharmacol Exp Ther* 2002, **301**(1):7–14.
14. Sisodiya SM, Lin WR, Harding BN, Squier MV, Thom M: **Drug resistance in epilepsy: expression of drug resistance proteins in common causes of refractory epilepsy.** *Brain* 2002, **125**(Pt 1):22–31.
15. Rizzi M, Caccia S, Guiso G, Richichi C, Gorter JA, Aronica E, Aliprandi M, Bagnati R, Fanelli R, D'Incalci M, Samanin R, Vezzani A: **Limbic seizures induce P-glycoprotein in rodent brain: functional implications for pharmacoresistance.** *J Neurosci* 2002, **22**(14):5833–5839.
16. Uchida Y, Ohtsuki S, Katsukura Y, Ikeda C, Suzuki T, Kamiie J, Terasaki T: **Quantitative targeted absolute proteomics of human blood–brain barrier transporters and receptors.** *J Neurochem* 2011, **117**(2):333–345.
17. Syvänen S, Lindhe O, Palner M, Kornum BR, Rahman O, Langstrom B, Knudsen GM, Hammarlund-Udenaes M: **Species differences in blood–brain barrier transport of three positron emission tomography radioligands with emphasis on P-glycoprotein transport.** *Drug Metab Dispos* 2009, **37**(3):635–643.
18. Bauer M, Zeitlinger M, Karch R, Matzneller P, Stanek J, Jager W, Bohmdorfer M, Wadsak W, Mitterhauser M, Bankstahl JP, Löscher W, Köpp M, Kuntner C, Müller M, Langer O: **Pgp-mediated interaction between (R)-[11C] verapamil and tariquidar at the human blood–brain barrier: a comparison with rat data.** *Clin Pharmacol Ther* 2012, **91**(2):227–233.
19. Abanades S, van der Aart J, Barletta JA, Marzano C, Searle GE, Salinas CA, Ahmad JJ, Reiley RR, Pampols-Maso S, Zamuner S, Cunningham VJ, Rabiner EA, Laruelle MA, Gunn RN: **Prediction of repeat-dose occupancy from single-dose data: characterisation of the relationship between plasma pharmacokinetics and brain target occupancy.** *J Cereb Blood Flow Metab* 2011, **31**(3):944–952.
20. Kim E, Howes OD, Kim BH, Yu KS, Jeong JM, Lee JS, Kim SJ, Jang IJ, Park JS, Kim YG, Shin SG, Turkheimer FE, Kapur S, Kwon JS: **The use of healthy volunteers instead of patients to inform drug dosing studies: a [(1)(1)C] raclopride PET study.** *Psychopharmacology (Berl)* 2011, **217**(4):515–523.
21. Liefaard LC, Ploeger BA, Molthoff CF, Boellaard R, Lammertsma AA, Danhof M, Voskuyl RA: **Population pharmacokinetic analysis for simultaneous determination of B (max) and K (D) in vivo by positron emission tomography.** *Mol Imaging Biol* 2005, **7**(6):411–421.
22. Liefaard LC, Ploeger BA, Molthoff CF, de Jong HW, Dijkstra J, van der Weerd L, Lammertsma AA, Danhof M, Voskuyl RA: **Changes in GABAA receptor properties in amygdala kindled animals: in vivo studies using [11C]flumazenil and positron emission tomography.** *Epilepsia* 2009, **50**(1):88–98.
23. Lim KS, Kwon JS, Jang IJ, Jeong JM, Lee JS, Kim HW, Kang WJ, Kim JR, Cho JY, Kim E, Yoo SY, Shin SG, Yu KS: **Modeling of brain D2 receptor occupancy-plasma concentration relationships with a novel antipsychotic, YKP1358, using serial PET scans in healthy volunteers.** *Clin Pharmacol Ther* 2007, **81**(2):252–258.
24. Syvänen S, de Lange EC, Tagawa Y, Schenke M, Molthoff CF, Windhorst AD, Lammertsma AA, Voskuyl RA: **Simultaneous in vivo measurements of receptor density and affinity using [11C]flumazenil and positron emission tomography: comparison of full saturation and steady state methods.** *Neuroimage* 2011, **57**(3):928–937.
25. Syvänen S, Hooker A, Rahman O, Wilking H, Blomquist G, Langstrom B, Bergstrom M, Hammarlund-Udenaes M: **Pharmacokinetics of P-glycoprotein inhibition in the rat blood–brain barrier.** *J Pharm Sci* 2008, **97**(12):5386–5400.
26. Syvänen S, Luurtsema G, Molthoff CF, Windhorst AD, Huisman MC, Lammertsma AA, Voskuyl RA, de Lange EC: **(R)-[11C]verapamil PET studies to assess changes in P-glycoprotein expression and functionality in rat blood–brain barrier after exposure to kainate-induced status epilepticus.** *BMC Med Imaging* 2011, **11**:1.
27. van Rij CM, Huitema AD, Swart EL, Greuter HN, Lammertsma AA, van Loenen AC, Franssen EJ: **Population plasma pharmacokinetics of 11C-flumazenil at tracer concentrations.** *Br J Clin Pharmacol* 2005, **60**(5):477–485.
28. Zamuner S, Gomeni R, Bye A: **Estimate the time varying brain receptor occupancy in PET imaging experiments using non-linear fixed and mixed effect modeling approach.** *Nucl Med Biol* 2002, **29**(1):115–123.
29. Zamuner S, Rabiner EA, Fernandes SA, Bani M, Gunn RN, Gomeni R, Ratti E, Cunningham VJ: **A pharmacokinetic PET study of NK receptor occupancy.** *Eur J Nucl Med Mol Imaging* 2012, **39**(2):226–235.
30. Wagner CC, Bauer M, Karch R, Feurstein T, Kopp S, Chiba P, Kletter K, Loscher W, Muller M, Zeitlinger M, Langer O: **A pilot study to assess the efficacy of tariquidar to inhibit P-glycoprotein at the human blood–brain barrier with (R)-11C-verapamil and PET.** *J Nucl Med* 2009, **50**(12):1954–1961.
31. Syvänen S, Blomquist G, Sprycha M, Höglund AU, Roman M, Eriksson O, Hammarlund-Udenaes M, Langström B, Bergström M: **Duration and degree of cyclosporin induced P-glycoprotein inhibition in the rat blood–brain barrier can be studied with PET.** *Neuroimage* 2006, **32**(3):1134–1141.
32. Bankstahl JP, Kuntner C, Abrahim A, Karch R, Stanek J, Wanek T, Wadsak W, Kletter K, Müller M, Löscher W, Langer O: **Tariquidar-induced P-glycoprotein inhibition at the rat blood–brain barrier studied with (R)-11C-verapamil and PET.** *J Nucl Med* 2008, **49**(8):1328–1335.
33. Gunn RN, Gunn SR, Cunningham VJ: **Positron emission tomography compartmental models.** *J Cereb Blood Flow Metab* 2001, **21**(6):635–652.
34. Logan J: **Graphical analysis of PET data applied to reversible and irreversible tracers.** *Nucl Med Biol* 2000, **27**(7):661–670.
35. Jonsson EN, Karlsson MO: **Xpose–an S-PLUS based population pharmacokinetic/pharmacodynamic model building aid for NONMEM.** *Comput Methods Programs Biomed* 1999, **58**(1):51–64.
36. Wilkins JJ: **NONMEMory: a run management tool for NONMEM.** *Comput Methods Programs Biomed* 2005, **78**(3):259–267.
37. Pillai G, Mentre F, Steimer JL: **Non-linear mixed effects modeling—from methodology and software development to driving implementation in drug development science.** *J Pharmacokinet Pharmacodyn* 2005, **32**(2):161–183.
38. Davies B, Morris T: **Physiological parameters in laboratory animals and humans.** *Pharm Res* 1993, **10**(7):1093–1095.
39. Dayneka NL, Garg V, Jusko WJ: **Comparison of four basic models of indirect pharmacodynamic responses.** *J Pharmacokinet Biopharm* 1993, **21**(4):457–478.
40. Higgins CF, Gottesman MM: **Is the multidrug transporter a flippase?** *Trends Biochem Sci* 1992, **17**(1):18–21.

doi:10.1186/2191-219X-2-58
Cite this article as: Müllauer *et al.*: Pharmacokinetic modeling of P-glycoprotein function at the rat and human blood–brain barriers studied with (*R*)-[^{11}C]verapamil positron emission tomography. *EJNMMI Research* 2012 **2**:58.

Submit your manuscript to a SpringerOpen journal and benefit from:

► Convenient online submission
► Rigorous peer review
► Immediate publication on acceptance
► Open access: articles freely available online
► High visibility within the field
► Retaining the copyright to your article

Submit your next manuscript at ► springeropen.com